Fixed-node Monte Carlo study of the two-dimensional Hubbard model

Guozhong An and J. M. J. van Leeuwen
Instituut-Lorentz, University of Leiden, P.O. Box 9506, 2300 RA Leiden, The Netherlands
(Received 18 March 1991)

The fixed-node Monte Carlo method is extended to lattice fermion models. This method replaces the problem of finding the ground state of a many-fermion system by an effective eigenvalue problem of finding the lowest-energy wave function in a given region of the configuration space. It has previously only been applied to fermions moving in continuous space. The discreteness of the configuration space causes the algorithm to differ from that of the continuum. The method is tested against a known limiting case where exact results are available for comparison. Good agreement is found. Using the fixed-node Monte Carlo method, we study the domain-wall phase in the ground state of the two-dimensional Hubbard model. The existence of a domain-wall phase which has domains of antiferromagnetic phases separated by walls of holes is recently suggested by inhomogeneous Hartree-Fock (HF) and variational Monte Carlo (VMC) calculations. Large improvements of the energies are found. The domain walls are broader than those obtained by the HF and VMC calculations.

I. INTRODUCTION

Numerical methods become increasingly important in the understanding of the physical properties of strongly correlated fermion systems where traditional perturbation approaches fail. The simplest model of a strongly correlated electron system is perhaps the Hubbard model. The Hamiltonian takes the form

$$H=-\sum_{\mathbf{r}\mathbf{r}'\sigma} t_{\mathbf{r}\mathbf{r}'} c^{\dagger}_{\mathbf{r}\sigma} c_{\mathbf{r}'\sigma} + U \sum_{\mathbf{r}} n_{\mathbf{r}\uparrow} n_{\mathbf{r}\downarrow} , \tag{1}$$

where $t_{\mathbf{r}\mathbf{r}'}=t$, if $\mathbf{r}$ and $\mathbf{r}'$ are nearest neighbors and 0 otherwise. $c^{\dagger}_{\mathbf{r}\sigma}$ is the creation operator for position $\mathbf{r}$ with spin σ, and $n_{\mathbf{r}\sigma}=c^{\dagger}_{\mathbf{r}\sigma}c_{\mathbf{r}\sigma}$. Except in one dimension, the phase diagram of the model is still not fully determined in spite of the large amount of work devoted to it.

The Green-function Monte Carlo (MC) technique[1,2] is an exact numerical method for computing the ground-state energy. It does so by projecting out the excited states from an initial trial wave function which is not orthogonal to the ground state. For fermion systems this method is not directly applicable because of cancellations between positive and negative contributions in the evaluation of observables (the sign problem). The sign problem is a direct consequence of the presence of both positive and negative signs in the ground-state wave function of fermion systems. The fixed-node Monte Carlo (FNMC) idea[2] circumvents the sign difficulty by replacing the original fermion eigenvalue problem by a related one. The new problem seeks the lowest-energy state under the constraint that it does not change sign in a prescribed region, while the original problem seeks the lowest state with the fermion symmetry in the whole region. The nodal structure, i.e., the domains of fixed sign, has to be supplied by a trial wave function. The solution of the new problem provides a variational approximation to the original problem. Central to the FNMC method is the trial wave function. The FNMC method has previously only been developed for fermions moving in continuous space.[2]. We extend this method to lattice fermion systems.[1,15] The discreteness of the configuration space causes the algorithm to differ from that of the continuum.

Recent inhomogeneous Hartree-Fock (HF) calculations[3] and variational Monte Carlo (VMC) calculations[4] employing the Gutzwiller wave function suggest that the Hubbard model has a so-called domain-wall ground state rather than the conventional two-sublattice antiferromagnetic state when the electron density is different from one electron per site. The domain-wall phase consists of two-sublattice antiferromagnetic strips separated by walls of holes. Using the FNMC method, we study the domain-wall phase of the Hubbard model. The HF and VMC wave functions provide starting points for our FNMC calculation.

The paper is organized as follows. In Sec. II the HF approximation and the Gutzwiller wave function are discussed. The fixed-node Monte Carlo method as developed for lattice fermions is presented in Sec. III. The results obtained for the ground state of the Hubbard model are given in Sec. IV.

II. TRIAL WAVE FUNCTIONS

In this section we describe the determination of trial wave functions. Two types of trial wave functions will be used: the Hartree-Fock (HF) and the Gutzwiller wave function (GWF). The HF wave function is determined by the HF equations. The Gutzwiller wave function has to be determined by the variational Monte Carlo method.[5,6]

A. Hartree-Fock wave function

Substituting $n_{\mathbf{r}\sigma}=\langle n_{\mathbf{r}\sigma}\rangle+\delta_{\mathbf{r}\sigma}$ into (1) and keeping terms linear in $\delta_{\mathbf{r}\sigma}$, we have $H=H_{\mathrm{HF}}+E_0[n]+O(\delta_{\mathbf{r}\uparrow}\delta_{\mathbf{r}\downarrow})$, where

$$H_{\mathrm{HF}}=-\sum_{\mathbf{r}\mathbf{r}'\sigma} t_{\mathbf{r}\mathbf{r}'} c^{\dagger}_{\mathbf{r}\sigma} c_{\mathbf{r}\sigma} + U \sum_{\mathbf{r}\sigma} n_{\mathbf{r}\sigma} \langle n_{\mathbf{r}-\sigma}\rangle , \tag{2}$$

and $E_0[n]=-U\sum_{\mathbf{r}}\langle n_{\mathbf{r}\uparrow}\rangle\langle n_{\mathbf{r}\downarrow}\rangle$. To diagonalize (2), a new set of fermion operators is introduced:

$$c_{k\sigma}=\sum_{\mathbf{r}}M_{k\mathbf{r}}(\sigma)c_{\mathbf{r}\sigma} \ . \tag{3}$$

The matrix M is unitary such that the $\{c_{k\sigma}\}$ satisfy again fermion commutation relations. Substituting (3) into (2), the HF Hamiltonian H_{HF} will take the diagonal form in the $c_{k\sigma}$, i.e.,

$$H_{\mathrm{HF}}=\sum_{k,\sigma}\varepsilon(k,\sigma)n_{k\sigma} \tag{4}$$

provided that $M^*_{k\mathbf{r}}(\sigma)=\phi_{k\sigma}(\mathbf{r})$ is chosen as the solution of the following HF equation:

$$-\sum_{\mathbf{r}'}t_{\mathbf{r}\mathbf{r}'}\phi_{k\sigma}(\mathbf{r}')+U\langle n_{\mathbf{r},-\sigma}\rangle\phi_{k\sigma}(\mathbf{r})=\varepsilon(k,\sigma)\phi_{k\sigma}(\mathbf{r}) \ . \tag{5}$$

The ground-state energy is optimized when $\langle n_{\mathbf{r}\sigma}\rangle$ satisfies the self-consistency equation

$$\langle n_{\mathbf{r}\sigma}\rangle=\sum_{k}|\phi_{k\sigma}(\mathbf{r})|^2\langle n_{k\sigma}\rangle \ . \tag{6}$$

Equations (5) and (6) must be solved self-consistently. The ground state of H_{HF} is given by

$$|\Psi_{\mathrm{HF}}\rangle=\prod_{k=1}^{N_\uparrow}c^\dagger_{k\uparrow}\prod_{k=1}^{N_\downarrow}c^\dagger_{k\downarrow}|0\rangle \ , \tag{7}$$

where $N_\uparrow$ ($N_\downarrow$) is the number of up (down)-spin electrons and the product is carried over the states with the lowest energy $\varepsilon(k,\sigma)$. Since we will not discuss a ferromagnetic phase, we assume $N_\uparrow=N_\downarrow=N/2$, where N is the total number of electrons in the system. The wave function then has the familiar Slater-determinant form

$$\begin{aligned}\Psi_{\mathrm{HF}}(R)&=\langle R|\Psi_{\mathrm{HF}}\rangle\\&=\det[\phi_{k\uparrow}(\mathbf{r}_i)]\det[\phi_{k\downarrow}(\mathbf{r}_j)] \ ,\end{aligned} \tag{8}$$

where $|R\rangle=c^\dagger_{\mathbf{r}_1\uparrow}c^\dagger_{\mathbf{r}_2\uparrow}\cdots c^\dagger_{\mathbf{r}_N\downarrow}|0\rangle$ denotes a configuration state and the rows of the determinant are composed of the set of $N/2$ lowest k states. The total energy is given by

$$\begin{aligned}E_{\mathrm{HF}}&=\langle\Psi_{\mathrm{HF}}|H|\Psi_{\mathrm{HF}}\rangle/\langle\Psi_{\mathrm{HF}}|\Psi_{\mathrm{HF}}\rangle\\&=2\sum_{1}^{N_\uparrow}\varepsilon_k+E_0[n] \ .\end{aligned} \tag{9}$$

A complete solution of (5) and (6) for arbitrary $\langle n_{\mathbf{r}\sigma}\rangle$ is still a formidable task. Symmetry properties of the solution need to be assumed in order to make the problem tractable. One assumption is that $n_{\mathbf{r}}=n$, $m_{\mathbf{r}}=m$, which leads to the two sublattice antiferromagnetic solution, where $n_{\mathbf{r}}=\langle n_{\mathbf{r}\uparrow}+n_{\mathbf{r}\downarrow}\rangle$ is the number density and $m_{\mathbf{r}}=A(\mathbf{r})\langle n_{\mathbf{r}\uparrow}-n_{\mathbf{r}\downarrow}\rangle$ is the staggered magnetization. [$A(\mathbf{r})=1$ for one sublattice and -1 for the other.] This phase is commensurate with the lattice structure and possesses long-range order. Incommensurate antiferromagnetic solutions are explored only very recently.[3] A modulated one-particle wave function

$$\phi_{k\sigma}(\mathbf{r})=e^{ipy}u_\sigma(x) \tag{10}$$

is assumed instead of a sublattice structure for the incommensurate solutions. Combining (10) with (6), we have $n_{\mathbf{r}}$ and $m_{\mathbf{r}}$ depending only on the x coordinate; hence $n_{\mathbf{r}}=n(x)$, $m_{\mathbf{r}}=m(x)$. The coordinates are such that the y axis is parallel to the domain wall and the x axis is perpendicular to it. For $U>4t$ the domain wall prefers to lie along the diagonal direction of the square lattice in the HF and Gutzwiller VMC approximations.[3,4] The HF equation as given by (5) takes a simpler one-dimensional form for the ansatz (10):

$$\begin{aligned}-2t\cos p\,[u_\sigma(x+1)+u_\sigma(x-1)]\\+\frac{U}{2}[n(x)-(-1)^x\sigma m(x)]u_\sigma(x)=\varepsilon u_\sigma(x) \ .\end{aligned} \tag{11}$$

Note that $n(x+l)=n(x)$, $m(x+l)=-m(x)$, where l is the domain-wall separation (an even number of domain walls are needed to satisfy the periodic boundary conditions). If l is even, it is evident that $u_{-\sigma}(x)=u_\sigma(x+l)$. Equation (11) is a matrix eigenvalue equation of finite dimension for a finite system. It can be diagonalized numerically.

B. Gutzwiller wave function

The HF approximation neglects correlation effects as the interaction is replaced by an effective potential. It is not expected to be a good approximation for strongly interacting systems where the potential energy is comparable to the kinetic energy. One way of improving the HF wave function is to introduce on-site pair correlations into the wave function by the Gutzwiller procedure, which multiplies the HF wave function by a factor taking the correlations into account,[7]

$$\Psi_T(R)=g^{N_p(R)}\det[\phi_{k\uparrow}(r_i)]\det[\phi_{k\downarrow}(r_j)] \ , \tag{12}$$

where the $\phi_{k\sigma}$'s are the lowest $\varepsilon(k,\sigma)$ solutions of (5) and $N_p(R)$ is the number of double occupied sites in configuration R. To reduce the computational effort, the domain wall is parametrized as [4]

$$n_{\mathbf{r}}=1-\alpha\sum_{l}1/\cosh[(x-x_l)/\xi_\rho) \ , \tag{13}$$

$$m_{\mathbf{r}}=m\prod_{l}\tanh[(x-x_l)/\xi_\sigma] \ . \tag{14}$$

Instead of satisfying the self-consistency, the optimal wave function is found by minimizing the energy $E(g,m,\xi_\sigma,\xi_\rho)=\langle H\rangle_{\Phi_T}$ against the parameters g,m,ξ_σ,ξ_ρ by the variational Monte Carlo method. The parameter α is determined by the total number of electrons in the system.

Both the HF and VMC calculations are carried out on a rectangular strip cut along the diagonal of the infinite square lattice. We measure the length in units of $a/\sqrt{2}$, where a is the lattice constant of the square lattice. A system with dimensions 14×8 ($a\sqrt{2}\times a/\sqrt{2}$) is shown in Fig. 1. Periodic boundary conditions are applied on the x

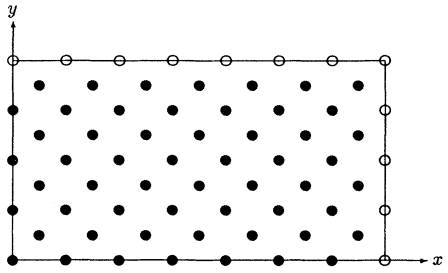

FIG. 1. 14×8 ($a/\sqrt{2}\times a/\sqrt{2}$) system. With periodic boundary conditions, the top row of sites is identical to the bottom row and the left row is identical to the right row. Note that the lattice is cut along the diagonal direction of the square lattice. Throughout this paper, the unit length is taken to be $a/\sqrt{2}$.

direction. Both periodic and antiperiodic boundary conditions are used in the y direction. For small L_y only a few wave vectors p are allowed. It is important to realize that for $p=\pi/2$ in Eqs. (10) and (11), all the single-particle wave functions $\phi_{k\sigma}$ are localized in the x direction. Therefore, a large portion of the electrons hop only along the y direction, which is untypical of larger systems. Antiperiodic (periodic) boundary conditions are needed in the y direction for systems with $L_y=4,8$ $(6,10)$ to avoid $p=\pi/2$ in Eq. (10).

The above-sketched idea regarding the boundary conditions is confirmed by numerical calculations. It is found that wave functions with periodic boundary conditions on the y direction for the system with $L_y=8$ are significantly higher in energy than those with antiperiodic boundary conditions. However, the energy is insensitive to the boundary conditions in the x direction. The variational energies under different boundary conditions are listed in Table I. The results for the antiperiodic-antiperiodic (aa) boundary conditions are that of Giamarchi and Lhuillier.[4] The variational parameters are chosen to be the optimal parameter under aa boundary conditions.

III. MONTE CARLO METHOD FOR LATTICE FERMIONS

The ground-state wave function Ψ_0 can be filtered out by applying a filter operator F to a trial wave function Ψ_T when $\langle\Psi_0|\Psi_T\rangle\neq0$. A particularly simple choice of a filter operator is $F=1-\tau_0(H-w)$,[1,8] where τ_0 and w are parameters to be specified. Let $\Psi^{(n)}=F^n\Psi_T$. We have

$$\lim_{n\to\infty}\Psi^{(n)}\to[1-\tau_0(E_0-w)]^n\Psi_0\langle\Psi_0|\Psi_T\rangle\ , \tag{15}$$

where E_0 is the exact ground-state energy. It is assumed that the ground-state wave function dominates over all the excited-state wave functions in (15). This requires

$$\tau_0<2/(E_{\max}+E_0-2w)\ , \tag{16}$$

where $E_{\max}$ is the maximum eigenvalue of H. The application of F on a wave function takes the form of matrix multiplication:

$$\begin{aligned}F\Psi(R)&=\sum_{R'}F(R,R')\Psi(R')\\&=(1+\tau_0 w)\Psi(R)-\tau_0\sum_{R'}H(R,R')\Psi(R')\ .\end{aligned} \tag{17}$$

For H given by (1), we have

$$H(R,R')=\begin{cases}UN_p(R), & R'=R\\ -t, & R'\in\mathcal{N}(R)\\ 0, & \text{otherwise}\ ,\end{cases} \tag{18}$$

where $\mathcal{N}(R)$ denotes the collection of configuration which can be reached from R by moving one electron to one of its nearest-neighbor sites. Equation (15) provides the basis for the exact evaluation of matrix element between the ground state and a trial state. Given an arbitrary operator O, we can express its action in configuration space:

$$\langle\Psi^{(n)}|O|\Psi_T\rangle=\sum_{R_n}\Psi^{(n)}(R_n)O\Psi_T(R_n)\ . \tag{19}$$

Define $O(R)\equiv O\Psi_T(R)/\Psi_T(R)$. Note that $O(R)$ is a function in R space and depends on the operator O and

TABLE I. Effects of boundary conditions on the energy. Energies obtained by the VMC method using the Gutzwiller wave function of the diagonal-wall type are given under various boundary conditions. The system has 112 sites and $N=104$ electrons. The dimension is 28×8 ($a/\sqrt{2}\times a/\sqrt{2}$). The energies and U are measured in units of t. The energy under periodic-antiperiodic (pa) boundary condition agrees with that under the antiperiodic-antiperiodic (aa) boundary condition within the error bar. [The data for the (aa) boundary condition are from Ref. 4.] The energy for periodic-periodic (pp) boundary condition is significantly higher than under the other two boundary conditions. The variational parameters are optimal for the (aa) boundary condition.

U	$-E$	$-E/N$	bc	m	ξ_ρ	ξ_σ	g
7	74.36(4)	0.7150	pp	0.28	3.4	3.2	0.45
7	75.70(5)	0.7279	pa	0.28	3.4	3.2	0.45
7	75.8(3)	0.728	aa	0.28(4)	3.4(4)	3.2(4)	0.45(2)
10	58.63(6)	0.5637	pp	0.26	3.4	2.8	0.35
10	59.42(6)	0.5714	pa	0.26	3.4	2.8	0.35
10	59.6(3)	0.573	aa	0.26(3)	3.4(3)	2.8(4)	0.35

the trial wave function Ψ_T. Substituting (17) into (19), we have

$$\langle \Psi^{(n)}|O|\Psi_T\rangle = \sum_{\mathcal{R}} O(R_n)\Psi_T(R_n) \times \prod_1^n F(R_i,R_{i-1})\Psi_T(R_0) , \quad (20)$$

where $\mathcal{R}=\{R_0,R_1,R_2,\ldots,R_n\}$ is a path in configuration space.

A. Nodeless wave function

Let us first look at the case for which Ψ_T has no sign change as for the ground-state wave function of a boson system. Equation (20) expresses a matrix element in terms of an enormous sum of known quantities in configuration space. This sum can be calculated by MC integration techniques. Since only part of the terms can be summed in a numerical calculation, it is highly desirable to select out those terms in the sum which have large contributions. This strategy is called importance sampling. It is accomplished by rewriting (20) as[1]

$$\langle \Psi^{(n)}|O|\Psi_T\rangle = \sum_R O(R_n)\prod_1^n G(R_i,R_{i-1})\Psi_T^2(R_0) , \quad (21)$$

where the Green function $G(R_2,R_1)=\Psi_T(R_2)F(R_2,R_1)\Psi_T^{-1}(R_1)$. The Green function G is factorized into a probability part and a weight part as

$$G(R_i,R_{i-1})=P(R_i,R_{i-1})m(R_i,R_{i-1}) , \quad (22)$$

with the normalization condition

$$\sum_{R_i} P(R_i,R_{i-1})=1 . \quad (23)$$

The importance sampling is achieved when paths $\mathcal{R}$ are generated according to the distribution $\prod_i P(R_i,R_{i-1})\Psi^2(R_0)$. The sum over the weights of all the generated paths gives the desired matrix element.

The ground-state energy can be evaluated exactly using the above strategy as

$$E_0=\langle \Psi_0|H|\Psi_T\rangle/\langle \Psi_0|\Psi_T\rangle = \frac{\sum_R W(R)E_L(R_n)}{\sum_R W(R)} , \quad (24)$$

where $W(R)=\prod_i m(R_i,R_{i-1})$. An approximate estimate for the ground-state average of any arbitrary observable can be obtained from[1,2]

$$\langle O\rangle \approx \langle \Psi_0|O|\Psi_T\rangle/\langle \Psi_0|\Psi_T\rangle . \quad (25)$$

B. Diffusion interpretation

The Monte Carlo process described above can be interpreted as searching for the stationary solution of a lattice diffusion equation by random walk and branching. From the definition of $\Psi^{(n)}$ and F, we have the following diffusion equation for $\Psi^{(n)}$:

$$\partial_t\Psi^{(n)}(R)= t\,\Delta\Psi^{(n)}(R) -[UN_p(R)-w-tzN]\Psi^{(n)}(R) , \quad (26)$$

where $\partial_\tau\Psi^{(n)}(R)=[\Psi^{(n+1)}(R)-\Psi^{(n)}(R)]/\tau_0$ and z is the number of nearest neighbors of a given lattice site. The Δ is the usual lattice Laplace operator:

$$\Delta\Psi(R)=\sum_\delta[\Psi(R+\delta)-\Psi(R)] , \quad (27)$$

where δ is the nearest-neighbor displacement vector which connects R to $R'\in\mathcal{N}(R)$. The appearance of the tzN term in (26) is caused by the subtractions in the lattice Laplace operator (27). The large n solution of (26) is the ground state of H.

The importance sampling replaces the diffusion equation for $\Psi^{(n)}$ by a generalized diffusion equation for $f^{(n)}(R)=\Psi^{(n)}(R)\Psi_T(R)$. From the definition of $G(R',R)$, we have

$$f^{(n+1)}(R)=\sum_{R'} G(R,R')f^{(n)}(R') . \quad (28)$$

Substituting the explicit expression for $G(R,R')$ and using (18), a generalized diffusion equation for $f^{(n)}(R)$ can also be derived:

$$\partial_\tau f^{(n)}(R)=[t\Delta-g(R)]f^{(n)}(R) +t\Psi_T(R)\sum_{a=\pm}\nabla_a f^{(n)}(R)\cdot\nabla_a\Psi_T(R)^{-1} , \quad (29)$$

where

$$g(R)=UN_p(R)-w-tzN-t\Psi_T(R)\Delta\Psi_T(R)^{-1}$$

and

$$\nabla_\pm f(R)=\sum_{\delta>0}[f(R\pm\delta)-f(R)] .$$

The forward (backward) difference operator ∇_+ (∇_-) appears because of the discrete nature of the diffusion process. The large n solution of (29) is given by $f^{(\infty)}(R)=\Psi^{(\infty)}(R)\Psi_T(R)$.

C. Fixed-node approximation

Since Ψ_T has both positive and negative signs for fermion systems, (21) is unsuitable for a MC evaluation. Following the idea of fixed-node MC approximation in continuous space,[2,9] we shall seek to solve an effective eigenvalue problem with nodeless wave functions. Important differences exist between the fixed-node MC approximation in continuous space and the one we shall develop. An eigenvalue problem for a nodeless wave function ψ is posed as follows:

$$\sum_{R'} H_{\text{eff}}(R,R')\psi(R')=\varepsilon\psi(R) , \quad (30)$$

where R is restricted to a set V of connected configurations inside which the trial wave function has the same sign. A natural choice for $H_{\text{eff}}(R,R')$ is

$$H_{\text{eff}}(R,R')=\begin{cases} H(R,R') & \text{if } R,R'\in V , \\ 0 & \text{otherwise} . \end{cases} \quad (31)$$

This is equivalent to setting $\psi(R)=0$ for $R\notin V$.[10] It is conceivable to use a more sophisticated H_{eff} than the simple choice (31). Ensembles of random walkers distributed according to the product of $\psi_T(R)$ and $\psi(R)$, which has the lowest ε, can be generated by the diffusion process outlined in Sec. III A. For the Hubbard model, (30) takes the form

$$-\sum_i \sum_{\mathbf{r}_i'} t_{\mathbf{r}_i\mathbf{r}_i'}\psi(\mathbf{r}_1',\mathbf{r}_2',\ldots,\mathbf{r}_N')+UN_p(R)\psi(R)=\varepsilon\psi(R)\ . \tag{32}$$

from (30) we conclude

$$H\psi(R)=\begin{cases}-t\displaystyle\sum_{R'\in\mathcal{N}(R)}\psi(R') & \text{if } R\in\partial V\ ,\\ \varepsilon\psi(R) & \text{otherwise}\ ,\end{cases} \tag{33}$$

where ∂V is the set of configurations which lie outside V and can reach configurations inside V by hopping one electron to one of its nearest-neighbor sites.

A variational wave function which has the correct fermion symmetry can be constructed from $\psi(R)$ as follows:

$$\hat{\psi}(R)=\sum_P(-1)^P\psi(r_{P1},r_{P2},\ldots,r_{PN})\ , \tag{34}$$

where P is a permutation of $(1,2,3,\ldots,N)$. We have $E=\langle H\rangle_{\hat{\psi}}\geq E_0$. However, the variational energy E cannot be evaluated easily. We approximate E by

$$E_F\equiv\frac{\sum_R\hat{\psi}(R)H\psi_T(R)}{\sum_R\hat{\psi}(R)\psi_T(R)}\ . \tag{35}$$

Using the fact that H is a Hermitian operator and (33) and (34), we have

$$E_F=\varepsilon+t\frac{\sum'_{R,R'}|\psi(R')\psi_T(R)|}{\sum_R\psi(R)\psi_T(R)}\ , \tag{36}$$

where the sum in the numerator of the second term is over all $R\in\partial V$ and $R'\in\mathcal{N}(R)$. Hence we have

$$E_F\geq\varepsilon\ . \tag{37}$$

This is in contrast to the continuum case[12] where $E=E_F=\varepsilon$. The above difference is caused by the fact the nodal surface for a lattice system may fall between configurations rather than on configurations.

D. Computational details

In the evaluation of the sum in (21), paths $\{\mathcal{R}\}$ distributed according to $\prod_i P(R_i,R_{i-1})\Psi_T^2(R_0)$ need to be generated. The paths $\{\mathcal{R}\}$ can be viewed as random walks in the configuration space. The random walkers are driven by the Green function to diffuse from the initial distribution $\Psi_T^2(R)$ to $\Psi_T(R)\Psi_0(R)$. A random walker at position R_{i-1} is moved to a new position R_i according to the probability $P(R_i,R_{i-1})$, where P is determined by (23) and (22). Further conditions are needed to specify P. For simplicity, we assume $m(R_i,R_{i-1})=m(R_{i-1})$. The normalization for P then implies

$$m(R_{i-1})=\sum_{R_i}G(R_i,R_{i-1})\ . \tag{38}$$

The discrete distribution $P(R_i,R_{i-1})$ is thus completely specified. The ratio of determinants appearing in G is calculated by a method described in Ref. 6. Zero probability is assigned to those positions which go beyond a nodal region.

The discrete distribution P is sampled by arranging it onto a line of unit length.[11] Each individual interval on the line represents the probability of a specific position. We generate a random number χ, which is distributed uniformly in the interval [0,1). The interval into which χ falls indicates the new position that the random walker is going to take. This gives the electron and direction in which the electron is to be moved.

The algorithm is summarized as follows

(1). Generate an initial ensemble of random walkers $\{R_i\}$ distributed according to $|\Psi_T(R)|^2$ by the variational Monte Carlo method.

(2). Propagate the random walkers in the ensemble one by one through s time steps until the whole ensemble is advanced by s time steps. This makes one interval.

(3). Do a death and birth process after each interval to increase the statistical efficiency. One simply replaces m by an integer $[m]=\lfloor m+\chi\rfloor$ (truncation), where χ is a random number uniformly distributed in the interval [0,1).

(4). Renormalize the ensemble size to its initial size after T intervals by randomly deleting and copying configuration. This completes a block.

The ensemble is chosen to contain about 1000 configurations. We compute as many blocks as the desired accuracy is achieved.

The parameter w in the filter operator F is adjusted to ε such that the average number of random walkers in each generation remains approximately constant. The basic time unit τ_0 is restricted by $\tau_0<1/(UN/2-w)$ such that $F(R,R)$ is positive. This is a more strict requirement on τ_0 than (16). The local energy $E_L(R)$ is measured throughout the random walks. The measurement of local energy in the initial block is discarded when the excited components are still present.

IV. RESULTS FOR THE HUBBARD MODEL

A. Comparison with exact results

To establish the accuracy of the approximation discussed in Sec. III C, we test it against the $U=0$ case of (1). This case is chosen because the exact wave function can be obtained easily. The system is oriented along (1,1) direction of the square lattice and has a dimension of 8×8 $(a/\sqrt{2}\times a/\sqrt{2})$. Periodic-antiperiodic boundary conditions are applied. The exact wave function is the paramagnetic solution of the HF equation, i.e., $n_{\mathbf{r}}=n$, $m_{\mathbf{r}}=0$ in (11).

The trial wave functions are constructed to be of the Gutzwiller form as given by (12). The determinant in (12) is chosen to be the exact wave function. The Gutzwiller

TABLE II. Comparisons between the fixed-node energy E_F and the exact energy E_{exact}. E_{GWF} is the energy of the Gutzwiller trial wave function. This system has 32 sites and 8 holes. The on-site interaction U is 0. The fixed-node energies are exact even with trial wave functions which give poor variational energies.

g	$-E_{\text{GWF}}$	$-E_F$	$-E_{\text{exact}}$	$-\varepsilon$
0.6	47.21(5)	50.48(3)	50.47	53.63(4)
0.7	48.83(3)	50.58(1)	50.47	53.66(3)
0.8	49.81(2)	50.45(2)	50.47	53.62(3)
0.9	50.32(1)	50.48(1)	50.47	53.67(3)

g factor controls the quality of the trial wave function without altering its nodal structure. Hence we expect that the nodal energy ε will not depend on the value of g, although E_F may. Energies obtained for g ranging from 0.6 to 0.9 are given in Table II. We see that indeed ε does not depend on g. However, it is surprising to see that the exact energy is achieved within the error bar even for a rather poor trial wave function with $g=0.6$.

B. Domain-wall phase

Calculations are performed on a 28×8 square lattice to study the stability of the domain wall phase at $U/t=7,10$. Only diagonal domain walls are considered since in the parameter range we study it is the most stable phase according to both HF and VMC results. The vertical domain-wall phase is expected to be the stable phase at $U/t<3.7$.[3] The number of holes in the system is such that there is one hole per site along the wall line. There are two domain walls in the system. The variational parameters for the Gutzwiller wave function are taken from Ref. 4 such that the results can be compared.

Our results are in qualitative agreement with the inhomogeneous HF and VMC calculations. The energies are significantly lower than those of the VMC and HF calculations. The energy difference between the domain-wall and commensurate phases is smaller than that obtained by VMC calculations. The VMC results are in between the HF and FNMC. Energies are given in Table III. One noticeable difference between our results and the VMC is the behavior of the hole condensation energy

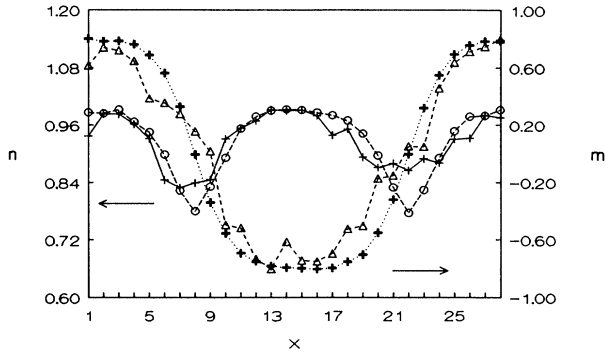

FIG. 2. Charge density (cross) and staggered magnetization (triangle) profiles for $U/t=7$. Also shown is the charge density (circle) and staaggered magnetization (bold cross) profiles from VMC calculations. The HF results, which are not shown in the figure, have the narrowest domain-wall structure. The lines are simply a guide to the eyes.

$E_c=E_{\text{CM}}-E_{\text{DW}}$ with U. Our results show that E_c is nearly the same for $U/t=7$ and 10. On the other hand, the VMC results show a monotonic increase of E_c from $U/t=0$ to $U/t=10$. For large U the Hubbard model close to half-filling can be mapped onto a t-J model with $J=2t/U^2$.[13] It behaves for large U as a weakly interacting system, excluding double occupied sites. Presumably the system then prefers to have a ferromagnetic ground state or even phase separation.[14] This may imply that E_c will first increase, reach a maximum, and then decrease to 0 with increasing U. Our results are consistent with the existence of a maximum for E_c between $U/t=7$ and 10.

The density profiles and staggered magnetization profiles are shown in Figs. 2 and 3. Two general features can be seen from our results. One is that the domain wall becomes narrower with increasing U. This feature, also present in the HF and VMC results, can be understood as follows. The shape of the domain wall is controlled by the competition between the loss of kinetic energy due to localizing the holes in the wall and the gain in potential energy from the antiferromagnetic ordering away from the wall. With increasing U/t, the potential energy be-

TABLE III. Ground-state energies obtained by the FNMC method for a $28\times 8(a/\sqrt{2}\times a/\sqrt{2})$ system. The system has 112 sites and 104 electrons. The trial wave functions used are GWF diagonal-wall (GWF DW), GWF, commensurate (GWF CM), and self-consistent HF diagonal-wall (HF DW) types. The fixed-node energies (E_F) are significantly lower than those obtained by the HF (E_{HF}) and the *VMC*(E_{GWF}) calculations. The diagonal domain-wall phase has energy lower than the commensurate phase for both $U/t=7$ and 10.

U	$-E_{\text{HF}}$	$-E_{\text{GWF}}$	$-E_F$	$-\varepsilon$	$-E_F/N$	*Type*
7	67.13		76.3(5)	77.9(9)	0.734	HF DW
7	67.13	75.70(5)	79.6(8)	84.6(2)	0.765	GWF DW
7	62.48	73.30(5)	78.5(1)	84.9(5)	0.755	GWF CM
10	51.77		59.4(3)	59.9(3)	0.571	HF DW
10	51.77	59.42(6)	64.3(2)	65.8(2)	0.618	GWF DW
10	45.87	54.46(5)	63.3(1)	66.4(2)	0.608	GWF CM

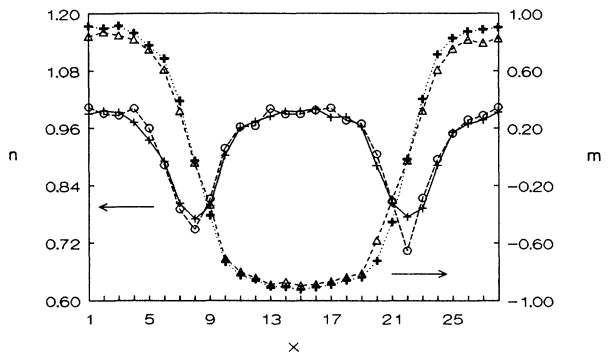

FIG. 3. Same as in Fig. 2 for $U/t=10$.

comes more important and narrower walls are favored. The second feature is that both HF and VMC results have walls narrower than the FNMC ones. This is due to the fact that both HF and VMC methods overestimate the effect of potential energy and underestimate the effect of kinetic energy.

To check the dependence of the results on the nodal structure of the trial wave function, the same system is studied using the self-consistent HF wave function as the trial wave function. Less satisfactory energy is obtained as shown in Table III. It means that the nodal structure of the self-consistent HF wave function is worse than the one provided by the Gutzwiller wave function, as specified by Eqs. (12)–(14).

V. DISCUSSION AND CONCLUSION

We have presented the extension of the fixed-node MC method for fermions to a lattice model for hopping fermions. Some of the extensions require only minor adaptations. The diffusion interpretation of the MC process is still valid as well as the projection technique to filter out the ground state. In lattice problems one does not need to make the short-time approximation for correct filtering. The random walkers diffuse according to probabilities dictated by the Green function and not with an *a priori* Gaussian distribution. The random walkers are not allowed to cross the boundaries of a nodal region. In the continuum case this has less consequences than in the lattice version. Restricting the wave function to one nodal region gives for the continuum case still the exact wave function (provided the nodal boundary is correct). Also, the kinetic energy, as a quasilocal operator, is only sensitive to the wave function inside a nodal region. So the extension of the wave function to the whole space by imposing the fermion symmetry is a formal operation which does not interfere with the ground-state energy calculation from the behavior in one nodal region.

The restriction to one nodal region does change the wave function for a lattice problem, since the nodal boundary is located between two configurations and the wave function does not vanish on either side of the boundary. Moreover, the kinetic-energy operator probes the wave function across the boundary, and so an extension of one nodal region to the whole space is not a pure formal operation, but does influence the kinetic-energy value. That this influence is substantial we see from the large difference between ε, the energy of the restricted problem, and E_F, which is a mixed estimate for the true problem.[12]

Thus it is surprising and reassuring that poor trial wave functions with exact nodal structure do give the exact value for E_F (within statistical accuracy), while the truncated value ε is quite far off (Table II). Therefore, we feel that also in lattice problems the main source of errors in the energy is caused by the nodal structure of the trial wave function.

We have applied the lattice FNMC method to study the incommensurate domain-wall phase in the two-dimensional Hubbard model. Our results agree qualitatively with VMC and HF calculations. Although the energy difference between the incommensurate domain-wall and commensurate phases is smaller than that obtained by the VMC calculation, it is large enough to see that the diagonal domain-wall phase is the stable one. The FNMC method can be used to study other types of phases as well. For example, one can use it to determine the phase boundary between the diagonal- and vertical-wall phases. Also, the method is by no means restricted to the Hubbard model.

Finally, we remark that the method developed here is complementary to the popular Trotter-formula approach[15] to quantum MC study of the lattice fermion models. The Trotter formula plus auxiliary- field approach is, in principle, exact; however, it is severely restricted by the sign problem. Our method is free from the sign problem and can be applied to relative large lattice sizes with moderate amount of computer time (all our simulations are done on a local network of SUN-SPARC work stations).

ACKNOWLEDGMENTS

We thank Berni Alder for initiating us into the present work and for a series of stimulating discussions. One of us (G.A.) is grateful to C. Lhuillier for discussions and correspondence regarding Ref. 4. We would also like to thank D. J. Bukman and P. J. H. Denteneer for useful comments to the manuscript. This research is supported in part by the Stichting voor Fundamenteel Onderzoek der Materie (FOM), which is financially supported by the Nederlandse Organisatie voor Wetenschappelijk Onderzoek (NWO).

[1] N. Trivedi and D. M. Ceperley, Phys. Rev. B **41**, 4552 (1990).

[2] P. J. Reynolds, D. M. Ceperley, B. J. Alder, and W. A. Lester, Jr., J. Chem. Phys. **77**, 5593 (1982); D. M. Ceperley and B. J. Alder, Phys. Rev. Lett. **45**, 566 (1980). For reviews of the Green-function MC and fixed-node MC applied to continuum case, see D. M. Ceperley and M. H. Kalos, in *Monte Carlo Methods in Statistical Physics*, edited by K. Binder (Springer-Verlag, Berlin, 1979); K. E. Schmidt and M. H. Kalos, in *Ap-*

pllications of the Monte Carlo Method in Statistical Physics, 2nd ed., edited by K. Binder (Springer-Verlag, Berlin, 1984).

[3]D. Poilblanc and T. M. Rice, Phys. Rev. B **39**, 9749 (1989); H. J. Schulz, J. Phys. (Paris) **50**, 2833 (1989); K. Machida, Physica C **158**, 192 (1989); J. Zaanen and O. Gunnarsson, Phys. Rev. B **40**, 7391 (1989).

[4]T. Giamarchi and C. Lhuillier, Phys. Rev. B **42**, 10 641 (1990).

[5]W. L. McMillan, Phys. Rev. **138**, A442 (1965).

[6]D. Ceperley, G. V. Chester, and K. H. Kalos, Phys. Rev. B **16**, 3081 (1977).

[7]M. C. Gutzwiller, Phys. Rev. Lett. **10**, 159 (1963); Phys. Rev. **137**, A1726 (1965).

[8]In continuous space, F would have to be chosen as $\exp(-\tau H)$ or $(H-w)^{-1}$ due to the need for F to be a bounded operator.

[9]D. J. Klein and H. M. Pickett, J. Chem. Phys. **64**, 4811 (1976).

[10]Other continuation of the wave function $\psi(R)$ outside the region V is conceivable. For example, one could take $\psi(R)=\psi_T(R)$ for $R\in V$. The problem is that we no longer have an eigenvalue equation.

[11]M. H. Kalos and P. A. Whitlock, *Monte Carlo Method: The Basics* (Wiley, New York, 1986).

[12]In the continuum case, we have $H\hat{\psi}(R)=\varepsilon\hat{\psi}(R)$, except on the nodal surface where $\psi_T(R)=0$. The second term in the right-hand side of (36) does not appear. Hence $E_F=\varepsilon=E$. The equality $E_F=E$ guarantees that E_F is an upper bound to the true ground-state energy, while in the discrete case (35) remains a so-called mixed estimator of the ground-state energy since H is sandwiched between two different states. A general inequality between E_F and the true ground-state energy could not be established in the discrete case.

[13]J. E. Hirsch, Phys. Rev. Lett. **54**, 1317 (1985).

[14]V. J. Emery, S. A. Kivelson, and H. Q. Lin, Phys. Rev. Lett. **64**, 475 (1990).

[15]For a review on the Trotter-formula plus auxiliary-field approach to the quantum MC study of lattice fermion systems and its problems, see H. De Raedt and W. von der Linden, in *The Monte Carlo Method in Condensed Matter Physics,* edited by K. Binder (Springer-Verlag, Berlin, in press).